

Global Ozone Monitoring Experiment ozone profile characterization using interpretation tools and lidar measurements for intercomparison

Y. J. Meijer,^{1,2} R. J. van der A,³ R. F. van Oss,³ D. P. J. Swart,¹ H. M. Kelder,^{2,3} and P. V. Johnston⁴

Received 12 February 2003; revised 16 August 2003; accepted 22 August 2003; published 6 December 2003.

[1] Global ozone profiles are derived from the ultraviolet and visible part of the spectra of the nadir-viewing Global Ozone Monitoring Experiment (GOME), which is mounted on the polar orbiting second Earth Remote Sensing satellite (ERS-2). These profiles need to be characterized, especially since the product includes a priori knowledge and so-called averaging kernels. This additional information needs to be taken into account when comparing the profiles to correlative measurements. We perform an intercomparison between the ground-based stratospheric lidar system in Lauder, New Zealand, and collocated GOME data. Here, the satellite profiles are retrieved with the algorithm of the Royal Netherlands Meteorological Institute (KNMI), which uses the optimal estimation method. In the comparison study significant differences are revealed which vary with season and altitude, indicating errors in the retrieval system. However, any quality assessment will just be one part of characterizing an ozone profile product that includes averaging kernels and a priori information. Data users need to be aware of the inherently complicated nature of such products that can only be fully understood when taking into account this additional information. In the second part of the study, the complex relation between the retrieved and the true profile is clarified using several interpretation tools. Applying these tools, we conclude that below 17-km altitude the GOME profiles can only be used with appropriate use of averaging kernels (e.g., in data assimilation). Above 17 km up to 50 km the GOME spectra contain useful profile information, but the retrieved profiles have a moderate vertical resolution of about 11 km and contain a substantial fraction of a priori information of about 50%. *INDEX TERMS:* 0340 Atmospheric Composition and Structure: Middle atmosphere—composition and chemistry; 0365 Atmospheric Composition and Structure: Troposphere—composition and chemistry; 0394 Atmospheric Composition and Structure: Instruments and techniques; 3360 Meteorology and Atmospheric Dynamics: Remote sensing; 3394 Meteorology and Atmospheric Dynamics: Instruments and techniques; *KEYWORDS:* GOME, remote sensing, ozone profile, lidar, validation, stratosphere

Citation: Meijer, Y. J., R. J. van der A, R. F. van Oss, D. P. J. Swart, H. M. Kelder, and P. V. Johnston, Global Ozone Monitoring Experiment ozone profile characterization using interpretation tools and lidar measurements for intercomparison, *J. Geophys. Res.*, 108(D23), 4723, doi:10.1029/2003JD003498, 2003.

1. Introduction

[2] Knowledge of the global distribution of ozone is of great importance for understanding the physical and chemical processes in the Earth's atmosphere. One of the major benefits of this knowledge will be to improve existing

climate and numerical weather models. Another important issue is to determine the anthropogenic effect on the ozone layer. There are several ways to measure ozone profiles, but the best way to get good global coverage is by using spaceborne sensors.

[3] The Global Ozone Monitoring Experiment (GOME) was launched on board the European Space Agency's (ESA) second Earth Remote Sensing satellite (ERS-2) in 1995 [Burrows *et al.*, 1999]. Its main objective is to retrieve atmospheric trace gas densities, but as the name suggests with a strong emphasis on ozone. GOME is a nadir-viewing spectrometer measuring the backscattered sunlight from the atmosphere in the wavelength range 240–790 nm. This information can be used to retrieve height-resolved ozone densities in the stratosphere as well as in the troposphere, which are based on the strong increase of absorption by ozone toward the shortest wavelengths. This method of ozone profile retrieval has been exploited previously by

¹Laboratory for Environmental Measurements, Environmental Risks and Safety Division, National Institute of Public Health and the Environment, Bilthoven, Netherlands.

²Also at Faculty of Applied Physics, Eindhoven University of Technology, Eindhoven, Netherlands.

³Section Atmospheric Composition, Department of Climate Research and Seismology, Royal Netherlands Meteorological Institute, De Bilt, Netherlands.

⁴National Institute of Water and Atmospheric Research, Lauder, Central Otago, New Zealand.

using data of the first and second Solar Backscatter Ultraviolet (SBUV and SBUV/2, respectively) satellite sensors [Bhartia *et al.*, 1996]. In the future, a whole set of similar instruments will succeed the GOME mission, namely Scanning Imaging Absorption Spectrometer for Atmospheric Cartography (SCIAMACHY, in 2002 on ENVISAT), Ozone Monitoring Instrument (OMI, in 2004 on EOS-AURA) and the GOME-2 series (from 2006 on METOP 1, 2, and 3), which stresses the need to characterize this type of measurement.

[4] Various ozone-profile retrieval algorithms for GOME data have been presented in the literature in recent years [Munro *et al.*, 1998; van der A *et al.*, 1998; Hoogen *et al.*, 1999; Hasekamp and Landgraf, 2001; Müller *et al.*, 2003], and most algorithms require that the observed spectra are absolute radiometrically calibrated with high accuracy. We have already demonstrated this importance of well-calibrated radiometric data [van der A *et al.*, 2002], and in this paper we will focus in more detail on the quality and characterization of the retrieved product presented in that paper. Note that the neural network approach presented by Müller *et al.* [2003] does not require this high accuracy of the calibrated spectra.

[5] Earlier GOME ozone-profile intercomparison studies of Hoogen *et al.* [1999] and Hasekamp and Landgraf [2001] used balloonsonde measurements, but the balloons are usually limited to 30-km altitude. We use high-quality lidar data from Lauder, New Zealand, to compare the ozone profiles. The altitude range of these data is 10–48 km, and we will demonstrate later that this covers the most useful part of GOME's altitude range. We have chosen to perform a detailed intercomparison study at one site, and in future studies we will expand the intercomparison to cover different global regions; in particular to include data from both hemispheres, including the tropics, and the polar regions.

[6] Although these studies aim to indicate the validity of the retrieval product, it can still be hard to fully understand the product itself, since it includes the so-called averaging kernels and a priori data. We therefore propose a set of diagnostic tools that should help to interpret the GOME ozone profiles. These tools are largely based on earlier, more theoretical, work of Rodgers [1990, 2000].

[7] In the following section we briefly present the GOME ozone-profile retrieval technique and the overall product, as it is used at the Royal Meteorological Institute (KNMI) in Netherlands. In section 3 we present a detailed intercomparison study in which we use lidar measurements, and in section 4 we separately present how to interpret the retrieved product. Finally, in section 5, we present a discussion and the conclusions of the results.

2. GOME Retrieval and Product Description

2.1. GOME Ozone-Profile Retrieval Technique

[8] Ozone profile information is contained in reflectance spectra in the near-ultraviolet wavelength region. Solar radiation, backscattered by air molecules, aerosols, and the surface, experiences a strong wavelength-dependent absorption by atmospheric ozone in the Hartley band (240–310 nm). At short wavelengths the absorption is so large that the atmosphere is opaque and the backscattered light observed by the satellite only originates from the

highest layers. At longer wavelengths the solar radiation penetrates deeper into the atmosphere and deeper layers start to contribute to the backscattered light. Since the amount of ozone in these layers is the main factor that determines how deep the sunlight reaches, combining measured reflectance in a suitable wavelength range gives the desired ozone profile information.

[9] The decreasing absorption of light toward longer wavelengths and the increase in the amount of ozone at lower levels almost balance each other and therefore the sensitivity of the retrieval system remains quite constant until the main ozone peak around 25-km altitude. The lower ozone concentrations below this altitude will hardly have any effect on the light observed by GOME. Therefore the retrieval for these levels gets increasingly more difficult, but can be slightly improved by taking into account the temperature dependence of ozone absorption in the Huggins band (310–340 nm) [Chance *et al.*, 1997; Munro *et al.*, 1998].

[10] The retrieval algorithm of KNMI uses the well-known nonlinear optimal estimation method of Rodgers [1990, 2000]. Rodgers outlines a method for solving underdetermined problems by using a priori information; a forward model relates the measurement to, in our case, the atmospheric profile elements. For underdetermined problems, like ozone profile retrieval from UV-reflectance measurements, normal least squares fitting does not work, since it amplifies measurement noise to unphysical, large-amplitude, profile elements. The use of an a priori profile tends to stabilize the inversion. In the KNMI retrieval algorithm (version 3.6), a priori ozone profiles are taken from the climatology of Fortuin and Kelder [1998] and the MODTRAN 3.7 radiative transfer model is used for the forward calculation. This algorithm and preliminary comparison results were previously published in a paper by van der A *et al.* [2002].

[11] The version 3.6 algorithm uses the spectral interval from 265 to 340 nm. Spectra are normally supplied by ESA through the GOME Data Processor (GDP) version 2.0. The ozone profile retrieval is highly dependent on the accuracy of the calibrated reflectivities. van der A *et al.* [2002] presented some case studies which demonstrated that differences between lidar and GOME data could be attributed to calibration errors in the GDP reflectivity spectra. In addition, comparison of many GDP reflectivity spectra with model results, by van der A *et al.* [2002], showed several systematic errors of these spectra, which was confirmed by comparisons made with spectra of the SBUV/2 satellite instrument. Corrections were proposed and have been applied to recalibrate GOME's measured reflectance. In this paper we will show a profile intercomparison using spectra including this recalibration as discussed by van der A *et al.* [2002].

2.2. GOME Ozone Profile Product of KNMI

[12] The final product of the ozone profile retrieval consists of ozone number densities on 11 pressure levels, the total column density of the Integrated Ozone Profile (GOME-IOP), and the so-called averaging kernel matrix. The pressure levels are 453, 218, 119, 60, 30, 16, 9, 5, 3, 1.7, and 1 mbar. The retrieved ozone profile from the optimal estimation method can be regarded as the a priori

profile updated with the profile information contained in the spectral measurement (“retrieved profile anomaly”). These retrieved values are therefore related to the difference between the true and the a priori profile (“true profile anomaly”). In general, these anomalies are not equal because the measurement is less sensitive to fine structures and the profile below the ozone is maximum. This is quantified by the following equation [Rodgers, 2000, p. 31, 1990]:

$$\mathbf{x}_{\text{retrieved}} = \mathbf{x}_{\text{a priori}} + \mathbf{A}(\mathbf{x}_{\text{true}} - \mathbf{x}_{\text{a priori}}). \quad (1)$$

[13] In this equation $\mathbf{x}_{\text{retrieved}}$, $\mathbf{x}_{\text{a priori}}$, and \mathbf{x}_{true} are vectors of ozone number densities at the pressure levels of the retrieval algorithm and they correspond to the values of the retrieved, a priori, and true state, respectively. \mathbf{A} is the so-called averaging kernel matrix, or model resolution matrix, and it consists in this case 11×11 elements, which results from the 11 retrieval levels.

[14] The averaging kernel constitutes a map between the true and retrieved anomaly. Its elements depend on (1) the sensitivity of the spectral measurement to the true profile, (2) the measurement errors, and (3) the a priori errors. They reflect (1) the limited sensitivity of the spectral measurement to fine-scale structures and the profile below the ozone maximum. In addition, the kernels are depending on errors (2) and (3), because for decreasing measurement errors the averaging kernel matrix tends to the identity matrix, while for increasing errors the matrix elements tend to zero. For the a priori errors it is the other way around. Therefore the behavior of the averaging kernels, and thereby the vertical resolution of the profile, depend on both the measurement error and the magnitude of the a priori errors. For example, smaller a priori errors give a poorer resolution.

[15] Equation (1) also quantifies the deviation between the true and the retrieved profile, and is especially of importance when comparing the retrieved profile to correlative measurements. Note the extreme cases that when (1) \mathbf{A} is the identity matrix: the retrieved and the true profiles are equal and (2) all elements of \mathbf{A} are zero: the retrieved profile equals the a priori. A detailed analysis of the averaging kernels of the 1997 GOME profiles is presented in section 4.

3. Intercomparison of GOME-Retrieved Ozone Profiles

[16] A complete validation of the GOME ozone profiles should cover all different measurement situations, such as differences in atmospheric conditions, solar zenith angle (SZA), and cloud cover. Before performing such an extended validation, we have chosen to do a more detailed validation at one site, intending to gain confidence in the present quality of the retrieval algorithm and the underlying GOME spectral measurements. In order to prevent any confusion with such a fully validated product, we will call this validation at one site an intercomparison. Correlative data used in the intercomparison should be reliable and of high quality.

[17] The Network for Detection of Stratospheric Change (NDSC) was established in 1991 to provide such a consistent, standardized set of long-term measurements of atmo-

spheric trace gases, particles, and physical parameters, via a network of globally distributed sites. One of its main objectives is to provide independent calibrations and validations of space-borne sensors of the atmosphere. The National Institute of Water and Atmospheric Research (NIWA) Lauder (45.04°S, 169.68°E), New Zealand, is one of the primary NDSC stations and it is the only site in the Southern Hemisphere midlatitude region.

[18] At NIWA Lauder the vertical distribution of ozone in the atmosphere is routinely monitored by three different instruments, each with its own advantages such as altitude range, temporal and vertical resolution. Balloon-borne ozone measurements started in 1986, in 1992 a microwave radiometer was installed, and since December 1994 routine measurements of stratospheric ozone have been performed using the Dutch stratospheric lidar system of the National Institute of Public Health and the Environment (RIVM). The advantage of using lidar data for the intercomparison is its relatively high altitude resolution of 2–5 km and its altitude range of 10–48 km that covers almost the complete (0–50 km) and best (17–50 km, demonstrated later) part of the GOME profile.

[19] The RIVM ground-based ozone lidar is an ultraviolet differential absorption laser (DIAL) system. Laser pulses are sent into the atmosphere at two wavelengths (308 and 353 nm). At 308 nm the light is more affected by ozone absorption than at 353 nm. Ozone profiles can be derived from the detected backscattered signals by applying the DIAL method. For a detailed system and retrieval description, see *Brinksma et al.* [2000]. Profiles are measured during nighttime in clear-sky conditions and range from 10- to 48-km altitude.

[20] Data quality is regularly monitored under the NDSC protocol [McDermid *et al.*, 1998a, 1998b]. The Lauder NDSC data are of high quality, and validation work showed that averaged lidar and sonde ozone profiles agreed to within 1.5% (20–35 km), while averaged lidar and SAGE II profiles agreed to within 2.5% at 20–35 km and to within 5% between 35 and 45 km. Between 12 and 20 km the deviation between averaged lidar and sonde profiles is smaller than 9% [Brinksma *et al.*, 2000].

[21] The retrieval scheme of KNMI, like all other GOME profile algorithms, does not use the GOME total column derived with the differential optical absorption spectroscopy (GOME-DOAS) technique [Burrows *et al.*, 1999] as a constraint. The GOME-IOP is therefore independent from the GOME-DOAS total column, though obtained from the same spectral data. As an independent intercomparison we compare the GOME-IOPs with total ozone column densities, measured in Lauder with Dobson spectrophotometer #72 (Lauder-Dobson). *Boyd et al.* [1998] mention in their introduction that the Lauder-Dobson has a maximum difference of 0.4% against the World Standard Dobson Instrument #83 (for direct Sun observations in February 1997).

3.1. Intercomparison Approach

[22] In the comparison of two quantities, it is important to ensure that they are compared on equal footing. Assuming that the true state of the atmosphere is represented by the measurement of the DIAL system, we have substituted the lidar profile for the vector \mathbf{x}_{true} in equation (1). The approach of applying equation (1) in an intercomparison

was first suggested by *Connor et al.* [1991]. The “retrieved” lidar profile is now referred to as “transformed” and compared to the GOME retrieved profile.

[23] We will have to set certain selection criteria in both space and time, in order to compare similar air masses and to justify applying equation (1). The GOME ground pixel covers an area of 960 by 100 km², east-west and north-south, respectively (see Figure 1). The retrieved ozone profile represents an average over this area. Since the ERS-2 satellite is in a Sun-synchronous orbit, passing the equator at a fixed time of 1030 LT, GOME is measuring in the area around Lauder at the end of local morning.

[24] We have defined collocation of a ground-based and a satellite measurement, when the center of the closest GOME ground pixel was within a 700-km radius around Lauder. In addition, we have required that each GOME and lidar profile can only be used once (i.e., the GOME and lidar data sets are bijective). Since the satellite orbit is almost exactly going from north to south, when GOME measures, these requirements result in a maximum difference of 2.0° in latitude and 8.6° in longitude (see Figure 1). For the time criterion we defined collocation when the lidar measurement was performed either the night before or after the late morning overpass, i.e., within 16 hours. These criteria are sufficient when the results are averaged, and proved useful in previous intercomparison studies [*Stratospheric Processes and their role in Climate (SPARC)*, 1998, section 2.4.2; *Brinkma et al.*, 2000].

[25] We have used one complete year of observations in order to include possible seasonal effects in the study. An ideal intercomparison period for both the lidar and GOME instrument is the year 1997. In this year there were 122 lidar observations evenly spread throughout the year and GOME Sun-normalized radiances did not yet suffer from degradation effects, which started in 1998 as demonstrated by *van der A et al.* [2002]. Another reason for choosing 1997 is that, especially in the austral winter and spring period, there were a relatively large number of anomalies in the measured ozone profiles with respect to climatology [*Brinkma et al.*, 1998, 2002; *Connor et al.*, 1999]. We can therefore check the sensitivity of the retrieval to changes in the normal, climatological, profile structure. The above mentioned selection criteria, for data of 1997, result in 111 collocated lidar-GOME pairs.

[26] In order to apply equation (1) to the lidar profiles, we need to regrid the lidar profile to the GOME profile sampling, i.e., as number density on 11 pressure levels. GOME data are retrieved at pressure levels, while lidar data are naturally retrieved at altitude levels. We therefore used cospatial and cotemporal temperature profiles, obtained from the National Centers for Environmental Prediction (NCEP) daily analysis, to convert pressure levels to altitude levels. It turns out that each of the levels has a separation of about 4 km. The lidar data, with an altitude resolution of about 2–5 km, have been averaged over a 3-km interval centered on the GOME level, and now represent the same 4-km thick levels due to the resolution; these data are now referred to as regridded. The transformed lidar data were calculated by substituting the regridded lidar data for x_{true} in equation (1).

[27] An example of intercomparison (date is 970312, yymmdd) is shown in Figure 2 (left) illustrating all the

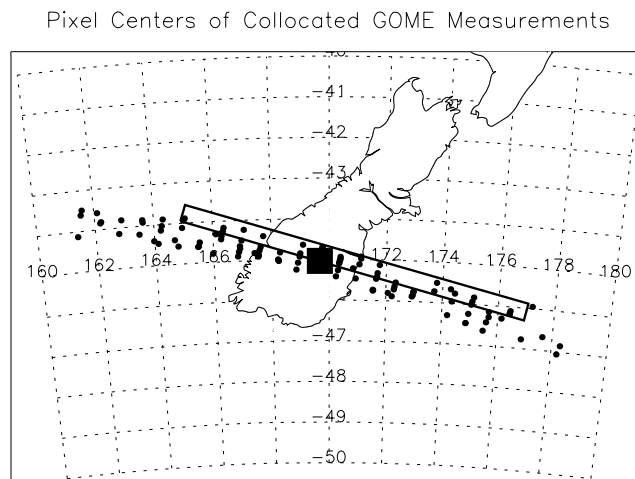


Figure 1. The rectangle illustrates the size of a single GOME ground pixel. The dots represent the centers of the 111 ground pixels of collocated GOME measurements used in this study. The solid square shows the geolocation of Lauder, New Zealand.

different profiles used, including the a priori and the original lidar ozone profile. The regridded lidar data are difficult to distinguish from the original lidar data, and their range is notably reduced due to the regridding. Actually, in general, it is difficult to compare profiles from such presentations and it is better to look at differences. Figure 2 (right) shows in terms of percentage the differences in ozone number density between both the GOME-retrieved and transformed lidar data, and a priori and regridded lidar data both relative to the lidar data. We need to use the regridded lidar data in the intercomparison with a priori data, because the a priori data used in the retrieval are also values representative for each GOME pressure level.

[28] In the retrieval the SZA is an important parameter and therefore we suspect that the retrieval might contain errors related to this. Throughout the year GOME measures at the same local time and therefore at different SZAs. In order to visualize systematic differences and to allow SZA-related effects to show up, we have calculated a 30-day running mean of the relative differences for a full year. An annual-mean relative difference would mask such effects. Note that other seasonally dependent errors, apart from solar zenith angle related errors, may also be possible.

3.2. Intercomparison Results of GOME Retrieval

3.2.1. Intercomparison of Ozone Profiles

[29] Initially, we focus on the actual state of the atmosphere in the chosen intercomparison period, because we can only see the added value of the GOME measurement if this state is substantially different from the climatology. Remember that climatological ozone profiles are used as the a priori state in the GOME retrieval and the values of these profiles are then adapted to optimally match the observed spectra. We therefore estimated the true profile anomaly during 1997, shown in Figure 3 (top). It shows in terms of percentage the 30-day running mean of the differences in ozone number density between the a priori data (climatol-

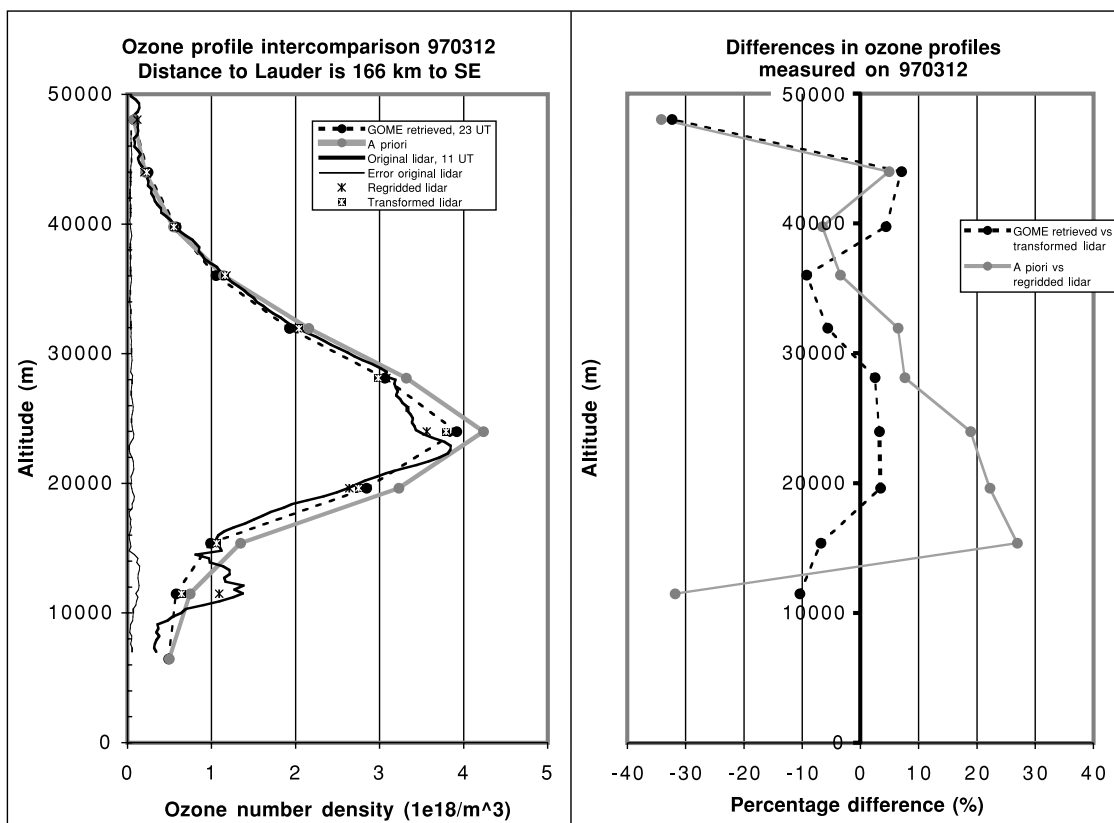


Figure 2. Example intercomparison of ozone profiles measured on 12 March 1997. (left) Retrieved GOME data (dashed line with dots), a priori data (shaded line with dots), transformed lidar data (squares with white asterisks), regridded lidar data (asterisks), original lidar data (solid line), and error original lidar data (thin solid line). (right) Differences between GOME and transformed lidar (dashed line with dots) and a priori data and regridded lidar data (shaded line with dots) in terms of percentage relative to the lidar. See text for definitions of regridded and transformed lidar data.

ogy) and regridded lidar data (actual state) relative to the latter. We can indeed (as mentioned in section 3.1) observe that from 1997.6 to 1997.8 the a priori values in the lower stratosphere are 20–30% higher than the actual state of the atmosphere, as represented by the regridded lidar data. We conclude that the year 1997 provides a good intercomparison data set in order to test the capabilities of the retrieval system.

[30] We now compare the GOME data, processed using the recalibrated GDP spectra, to lidar data, shown in Figure 3 (bottom). It shows in terms of percentage the 30-day running mean of the differences in ozone number density between the GOME data and transformed lidar data relative to the latter. A positive difference means that the retrieved GOME ozone number densities are higher than the transformed lidar observations. The observed mean differences range from -40 to $+40\%$, indicating errors in the retrieval system. Furthermore, these errors vary with season and altitude and are largest in the troposphere and lower stratosphere. We will discuss the possible cause of these errors in section 5.

[31] A bias smaller than 10% can be observed at the start and end of the year in the altitude range of 30–40 km, and even down to 17-km altitude in the middle of the year. However, these areas with a small bias will also be affected

when adjustments are made to compensate for the observed errors in the retrieval system. Typical values for the standard deviation of the mean differences are around 10% in the altitude range 15–45 km, and between 15 and 30% for the other altitudes, with the higher values in the middle of the year.

3.2.2. Intercomparison of Total Ozone Column Densities

[32] The previously defined selection criteria (section 3.1) have been applied to Lauder-Dobson and GOME data of 1997, with the additional criterion that the data should be measured on the same day. These criteria resulted in 177 collocated GOME-Dobson pairs.

[33] For each pair we calculated the difference in Dobson units (DU, $1 \text{ DU} = 0.001 \text{ atm cm}$) between the GOME-IOP and Lauder-Dobson values. We correlated the differences to the SZA, which is shown as a scatterplot in Figure 4. For clarity, an SZA of 32° corresponds to 21 December 1997 (austral summer solstice) and an SZA of 75° corresponds to 21 June 1997 (i.e., decimal date = 1997.45). A linear fit through these data is shown as a line in Figure 4. The calculated fit parameters, the mean of the differences and its standard deviation (1σ) are given in Table 1.

[34] Any seasonal dependent bias, including those depending on the SZA, can explain the derived SZA

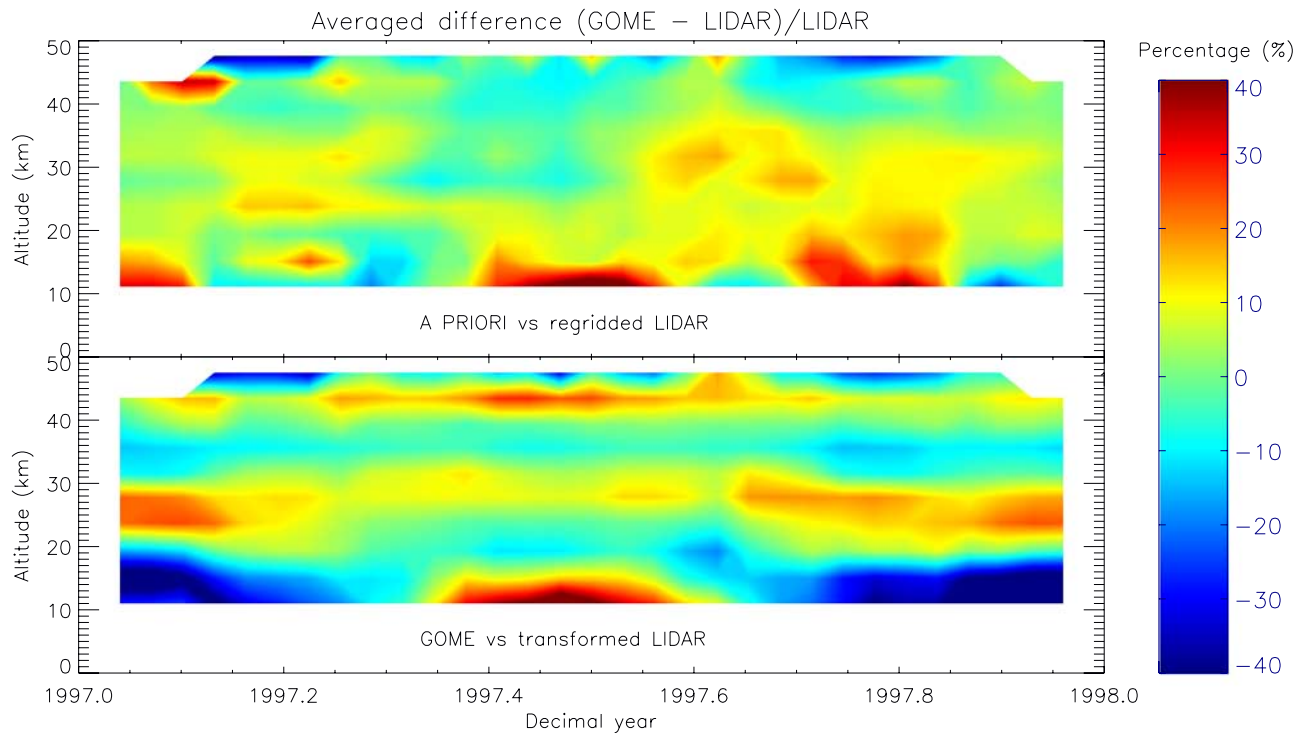


Figure 3. All relative differences in ozone number density in terms of percentage (such as in Figure 2) of the 111 GOME-lidar pairs for 1997 have been averaged by applying a 30-day running mean to each retrieval level. (top) Differences between a priori data and regridded lidar data. (bottom) Differences between the GOME-retrieved data and transformed lidar data. Gaps in top left and right corners correspond to missing data, and data lower than -40% or higher than $+40\%$ are plotted in the same color as -40 and $+40\%$.

correlation in the differences. In fact, part of the observed bias can be explained by a known systematic error in the Lauder-Dobson data, which *Brinksma et al.* [2000] demonstrated was due to the use of nontemperature-dependent Dobson ozone cross sections. Figure 8 of *Brinksma et al.* [2000] clearly shows the oscillating effect on the derived values when neglecting the seasonal dependence of this parameter. We derived an amplitude of about 3 DU from an update of this figure (E. J. Brinksma, personal communication, 2001), which introduces a seasonal dependent bias of the same sign as our C_1 fit parameter corresponding to about $0.15 \text{ DU}/^\circ \text{ SZA}$.

[35] The GOME-IOP has a slope of $0.66 \text{ DU}/^\circ \text{ SZA}$ that is about 4 times higher than expected from neglecting the known bias in the Lauder-Dobson data and about 11 times higher than the one-sigma error level of this slope. We conclude that the GOME-IOP is significantly seasonal dependent and that this dependence is consistent with the observed differences between the GOME and lidar data in the lower stratosphere (see Figure 3). The GOME ozone-profile retrieval algorithm uses temperature profiles based on climatological data of the European Centre of Medium-Range Weather Forecasts (ECMWF). The expected error in the ozone profile, due to the difference between the actual and climatological temperature profile, peaks in the troposphere with a few percent for a 5° temperature error. This error is not expected to be seasonal dependent and has little influence on the integrated ozone profile. Therefore tem-

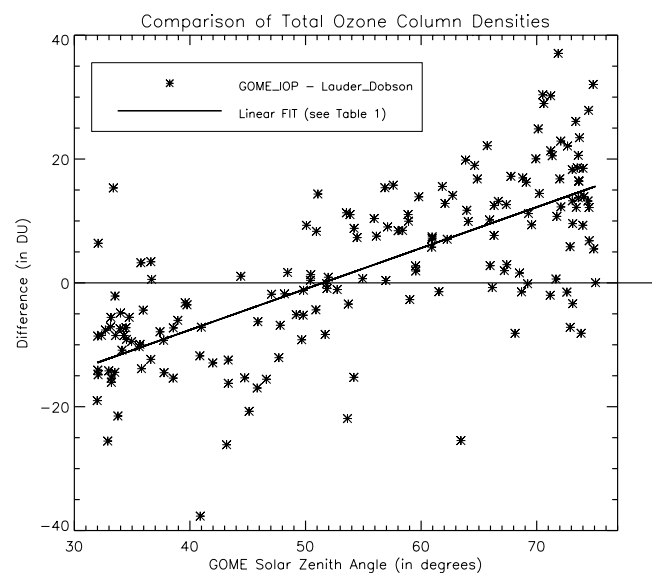


Figure 4. Differences in total ozone column densities in Dobson units (DU) between the GOME-integrated ozone profile (GOME_IOP) and data of the Lauder Dobson spectrophotometer (Lauder_Dobson) as a function of SZA. Plotted over the original data is a line fit (see Table 1 for fit parameters).

Table 1. Annual Mean Differences in Total Ozone Column Densities, and Fit Parameters of Linear Function (“GOME-IOP” - “Lauder-Dobson”) = $C_0 + C_1$ SZA

$C_0 \pm 1\sigma$, DU	$C_1 \pm 1\sigma$, DU/° SZA	Mean of Differences, DU	SD of Differences, DU
-34.0 ± 3.5	0.66 ± 0.06	2.6	15.2

perature effects cannot explain the large seasonal dependence observed in the GOME-IOP.

4. Interpretation of Retrieval of Nadir Ozone Profiles

[36] The intercomparison method of the previous section can be very helpful to improve a retrieval algorithm or to identify errors in the spectral measurements, but we have to be aware that it is not a conclusive validation method. The lidar data after transformation with equation (1) are no longer independent from the GOME-retrieved data. To understand what the capability of the observing system is to measure the true ozone profile is the main subject of the remainder of this paper.

[37] The retrieved product is referred to as an ozone profile, but this can be misleading. The term “profile” suggests height-resolved values of various layers. Lidar and sonde profiles usually give values at well-defined altitudes and they correspond to or are influenced by a certain confined altitude region which is symmetrically shaped around its nominal altitude; e.g., a Gaussian shape. This altitude region is referred to as vertical resolution, but for GOME profiles this region can be quite extensive, and also the functional relation between the retrieved value at one level and the true ozone profile at all levels can severely deviate from the expected shape.

[38] According to our experience there is a strong need for a better understanding of GOME’s ozone profile product. In order to understand this product we will have to analyze how the retrieved state is related to the true state of the atmosphere. For this we need to analyze the exact influence of the retrieval process, as quantified in equation (1). We would like to emphasize that this whole section deals with a subject quite different from that in section 3. It focuses on how to interpret a product that includes averaging kernels and a priori information. Though, if this additional information is incorporated when used, then there is no need for further interpretation; for example, when the data are applied in assimilation models.

[39] We would like to briefly summarize how averaging kernels and a priori information are used in data-assimilation models. The central quantities in data assimilation are the measurement error covariance matrix and the observation operator. The latter provides a model forecast of the observation based on the model state, or $\mathbf{x}_{\text{retrieved,model}} = \mathbf{H}[\mathbf{x}_{\text{forecast}}]$. This is of the same form as equation (1), with the true state replaced with the model forecast, and where \mathbf{H} contains the averaging kernel matrix and a priori information. The measurement error covariance comes from the ozone-profile retrieval error covariance matrix, but without the smoothing error [Rodgers, 2000, section 3.4.2]. These “retrieved model profiles” are then compared with the

GOME-retrieved profiles, and the model will adjust its values to optimally match the GOME measurements, meanwhile taking into account the measurement error and model forecast error covariance. Effectively, the assimilation model will only extract profile information from the measurement where it is present, which for each level is based on the kernel information and whether the measurement error is actually smaller than the model forecast error (for more details see, for example, Rodgers [2000, chapter 8]).

[40] As mentioned before, we believe that for most other applications there is a strong need for an easier, more physically oriented, interpretation. In the following part of this section we will therefore provide diagnostic tools, in order to make it easier to interpret the retrieved ozone profile. We will focus on three different aspects of the product, which are in essence described by equation (1). We will analyze in two ways how the averaging kernels have redistributed the values of the true state of the atmosphere. First, we will calculate the resolution of the product by estimating the resolution of the averaging kernels. Second, the retrieved values also tend to correspond to moving the true state ozone values either up or down. We will therefore raise the issue of what the corresponding altitude of the retrieved value actually is, compared to its nominal (reported) altitude. Finally, the amount of a priori information that is present in the retrieved product will be quantified.

[41] An example of a typical averaging kernel matrix for GOME retrieval near Lauder, New Zealand, in 1997, is shown in Figure 5. Note that traditionally each averaging

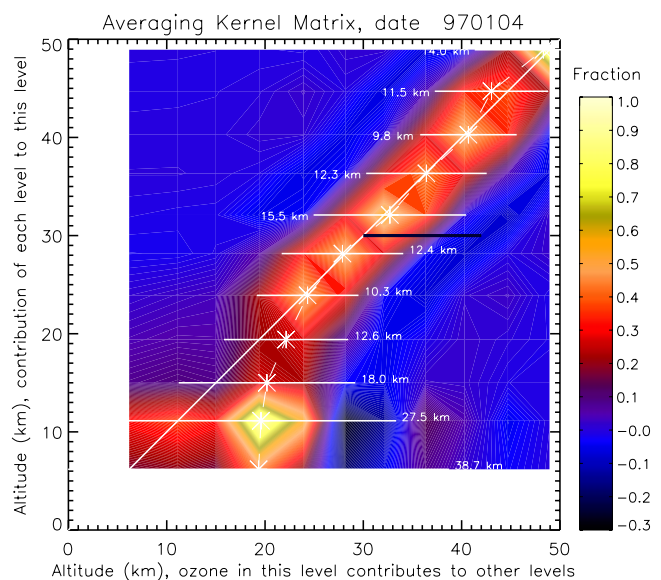


Figure 5. GOME averaging kernel matrix example (4 January 1997); rows are plotted horizontally and represent each kernel. Also shown are the centroid (asterisks) and the resolving length (horizontal lines, including its value) of each kernel. The black line indicates the distance between the maximum kernel value and the nearest minimum value higher up, which is also a kind of resolution of the retrieval system.

kernel is usually plotted as one line, corresponding to one horizontal line in Figure 5. Therefore the x axis shows how ozone at these levels contribute to ozone at the other levels and the y axis shows how much other levels contributed to the retrieved ozone value at that level. Note that, for example, a retrieved ozone value at about 10 km is largely dominated by ozone values around 20-km altitude. Averaging kernel matrices, like the one of Figure 5, will be used throughout the following sections and they are initially used to estimate the resolution of a kernel.

4.1. Averaging Kernels and Estimate of Resolution

[42] The most appropriate definition for resolution is a debatable subject and depends on the context of its application. Our aim is to apply a definition that gives a measure for the altitude range that contributes to the retrieved ozone value at a given retrieval altitude and that also accounts properly for contributions from negative lobes in the averaging kernels. In addition, we require that we can derive values for all levels, and we prefer to penalize odd-shaped kernels than to derive seemingly normal values. We have investigated several definitions, mentioned by *Rodgers* [1990, 2000, sections 3.3 and 3.4], which attempt to give a measure for the width of a kernel. Most of them give satisfying results at most altitudes, but they fail at certain levels that correspond to an odd-shaped kernel with, for example, a dislocated center or significant negative lobes. This happens when we applied full width at half maximum (FWHM), second moment about the mean altitude and second moment about the nominal altitude. In both manuscripts *Rodgers* also mentions a definition set up by *Backus and Gilbert* [1970], which they called “spread.” It gives satisfying results at all altitudes, but it also tends to severely penalize the kernels with dislocated centers. A related concept is the resolving length $r(z)$ or “spread about the center,” which is defined as

$$r(z) = 12 \frac{\int [z' - c(z)]^2 A^2(z, z') dz'}{\left(\int A(z, z') dz' \right)^2}, \quad (2)$$

where the center $c(z)$ is given by [*Rodgers*, 2000, p. 55 and 77]

$$c(z) = \frac{\int z' A^2(z, z') dz'}{\int A^2(z, z') dz'}. \quad (3)$$

In these equations z is the nominal altitude. The quantity $c(z)$ can be regarded as the centroid of a kernel, and this is the subject of the next section. The Backus–Gilbert spread is similar to the resolving length, but $c(z)$ is then replaced by z in equation (2). The factor 12 in equation (2) is chosen so that a simple slit function has a spread equal to its full width.

[43] We have chosen to apply equation (2) for estimating the kernel resolution, since it takes into account all the features that we wanted to be included in the definition of resolution. In this way we also separate the second feature

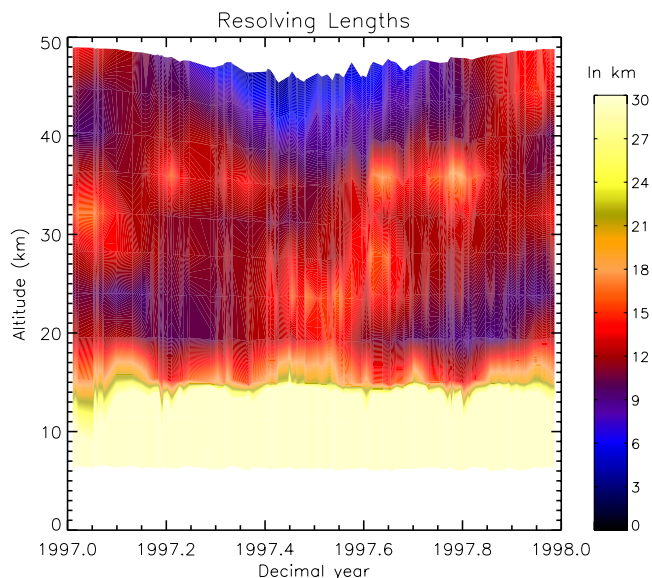


Figure 6. Resolving lengths calculated for all the 111 GOME averaging kernel matrices collocated with Lauder, New Zealand. Values larger than the maximum scale of the resolution are shown with the same color as 30 km.

of the averaging kernel, namely that in some cases it is not centered on its nominal altitude. In Figure 5 over the original data, we have plotted as an illustration for each kernel half the resolving length to either side of its centroid.

[44] The resolving lengths of all the averaging kernel matrices used in the 1997 intercomparison (see section 3) are shown in Figure 6. The average resolving length above 17-km altitude is 11.3 ± 2.6 km. At these altitudes the averaging kernel has its centroid more or less at the nominal altitude, as we will show in the next section. In this case the resolving lengths are about 25% higher than what would be found with the FWHM definition of resolution. In the same altitude range, *Hoogen et al.* [1999] found for their retrieval algorithm (northern mid-latitude winter scenario, SZA = 70°) an FWHM of about 9 km, which would correspond to very similar resolving lengths. Below about 17-km altitude the resolving lengths rapidly increase to more than 30 km and out of the plotting range, and they correspond to very odd-shaped kernels (for example, see lowest two levels in Figure 5). These, sometimes ridiculously, large values can be used to identify such kernels, but do not represent any useful value for its width. It is interesting to see in Figure 6 that in the middle of the year, when the SZA is large, the retrieval system can, as expected, achieve a better vertical resolution at the highest altitudes.

[45] In Figure 5 a feature is showing up in which a layer of negative kernel values is above the layer of the maximum kernel values. Each distinct layer of the retrieval system should be anticorrelated with the layer above it, because extra or too little absorption by ozone one layer higher has to be compensated for lower down. The capability of the retrieval system to discriminate between two independent layers can be looked upon as another definition of resolution. In Figure 5 at 30-km altitude, we estimate this distance to be about 12 km (see black line),

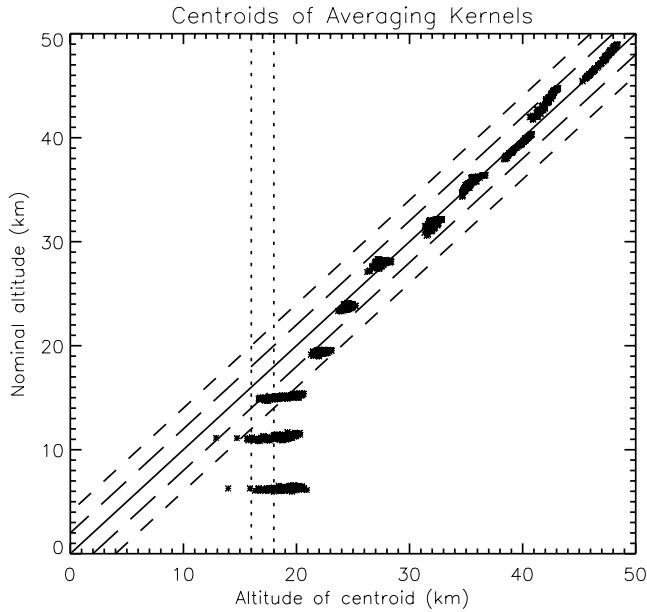


Figure 7. Centroids calculated for all the 111 GOME averaging kernel matrices as a function of their nominal altitude. Lines parallel to the diagonal show where the thresholds are for allowing a shift of 2 and 4 km (long and short dashed lines, respectively) away from the nominal altitude. Dotted lines show the minimum (left) and mean (right) penetration depth of the retrieval based on these centroids.

which is consistent with the average resolving length in this altitude range.

4.2. Altitude of Retrieved Value

[46] Kernels can have a centroid away from its nominal altitude and therefore the retrieved values relate to a dislocated true ozone profile. This can quite clearly be seen (in Figure 5) from the kernels at the lower levels, which all have their centroid around 20-km altitude. The interpretation of this is that almost all of the information attributed to this lower region is coming from the region around 20-km altitude.

[47] The centroids of all the kernels used in the 1997 intercomparison (see section 3) are shown in Figure 7. We have plotted the results in a similar way as in Figure 5, with the nominal altitude on the y axis. We have also plotted long dashed and short dashed lines that correspond to accepting a shift of ± 2 and 4 km, respectively, which would be more or less half and once the sampling interval of the retrieval system.

[48] There are almost no kernels with a centroid lower than 16-km altitude, and the average lower boundary is about 18 km. We already predicted this in section 2.1, because it is quite difficult to detect ozone below the main ozone peak, which is around 25-km altitude. Therefore the concentrations and fluctuations of ozone around 20-km altitude dominate the ozone concentrations retrieved for the troposphere and lower stratosphere.

[49] There are two exceptions that result in a centroid below 16-km altitude. The first type is connected to very low stratospheric ozone concentrations in early August

1997, as referred to in section 3.1. The other is due to high ozone concentrations around 11-km altitude and normal to low concentrations higher up. Because of these circumstances lower altitude levels become better observed, which in turn gives properly shaped averaging kernels and therefore less dislocated centroids.

[50] We argue that the centroid of a kernel can be used to reject certain retrieval levels, because sometimes a centroid is too far away from the nominal altitude. If a shift of one sampling interval is accepted, then only the profile levels above 14 km should be given. However, when this constraint is tightened to allow shifts of just half of the sampling interval, then sensible ozone values can be reported only above 20-km altitude.

4.3. Contribution of a Priori Information

[51] The retrieval of ozone profile information is an underdetermined problem which was treated by using the optimal estimation method. Care has to be taken that this involves the use of a priori profile information (see section 2). Equation (1) describes the dependence of the retrieved product on this a priori knowledge. Here, we will estimate how large the a priori contribution is.

[52] We have to separate two parts in which the a priori contributes to the retrieved value of a level z_i . The main contribution results from the diagonal element of the averaging kernel matrix, namely a fraction of $(1 - A_{ii})$ of a priori information. This fraction is added to a fraction of A_{ii} of true information at that level. In addition, the off-diagonal elements of the averaging kernel matrix contribute to the retrieved value, but they operate on the difference between the true and a priori state vectors and therefore form a smaller part of the final retrieved value of level z_i . All together it is quite complex to estimate the total fraction of a priori information, especially since it depends on the values of both state vectors. Therefore it is an easier approach to

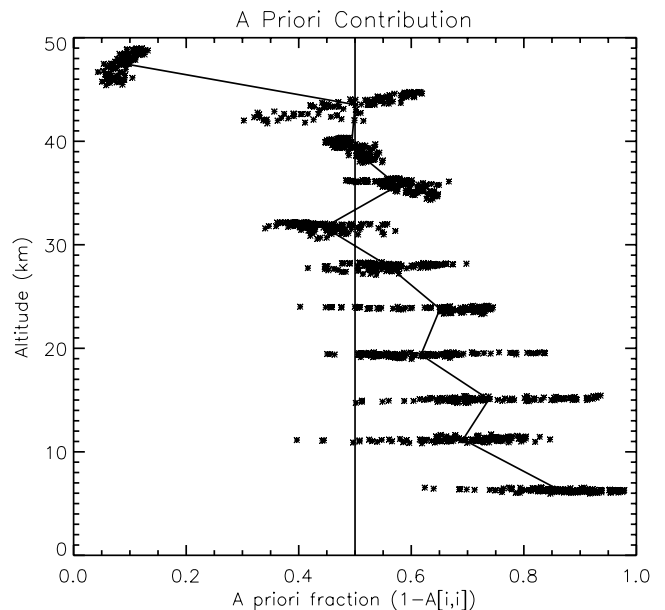


Figure 8. A priori ozone profile contribution to each retrieval level (asterisks) and its average values (solid line) for all collocated GOME measurements in 1997.

just examine the main fraction resulting from the diagonal elements of the averaging kernel matrix. This approach can be justified, since large off-diagonal contributions will also result in a shifted centroid, and in that case we stated earlier to reject the retrieved values from these levels. We therefore define the a priori contribution to each retrieval level z_i as the $(1 - A_{ii})$ fraction of the corresponding kernel.

[53] In Figure 8 we present the a priori contributions from the retrievals used in the 1997 intercomparison (see section 3). Up to 20-km altitude the a priori fraction is larger than the information of the true state of the atmosphere. Above this altitude the a priori knowledge still has a significant contribution (about 50%), except for the highest level.

5. Discussion and Conclusions

[54] Characterization of ozone profiles retrieved from spectral measurements of the GOME satellite instrument was the focus of this paper. We monitored the present quality of these profiles and the underlying GOME spectral measurements by comparing them with year-round, collocated lidar ozone profiles over Lauder, New Zealand, from 1997. In addition, the complex relation between the retrieved and the true profile, as quantified in the averaging kernels and the a priori profile, was clarified using several interpretation tools.

[55] *van der A et al.* [2002] demonstrated that the spectral measurements of GOME contain severe errors, which have a large effect on the retrieved ozone profiles. The recalibration used in the retrieval actually mainly affects the shorter wavelengths (<305 nm), with correction factors on the order of 0.9, which results in lower reflectivities at these wavelengths, and this translates into higher ozone values above ~ 30 km. Figure 3 (bottom) illustrates that the GOME profile retrieval system (algorithm and spectral measurements) still contains errors, and that they vary with season and altitude. Furthermore, these errors are largest in the troposphere and lower stratosphere.

[56] The revealed biases are significantly correlated to the solar zenith angle of observation, which demonstrates that there is a seasonal dependent bias, and this can be seen in both the comparison results of the ozone profiles and the total ozone column densities. Close examination of the figures of *Hoogen et al.* [1999, Figures 6 and 7] and *Hasekamp and Landgraf* [2001, Figures 9 and 13] show intercomparison results with similar errors for their retrieval algorithms. *Spurr* [2001, Figure 5.9] demonstrates that the origin of these errors might be in the neglect of polarization in the radiative transfer computation using MODTRAN. This neglect causes profile errors of up to 50% in the troposphere and lower stratosphere, and moreover, is dependent on the SZA. Also, *Hasekamp et al.* [2002] investigated the need of polarization modeling for ozone profile retrieval from backscattered sunlight. They showed the effect of an insufficient correction for the polarization sensitive instrument and of the use of the scalar approximation in the atmospheric radiative transfer model. The errors in the retrieved profiles arising from these effects strongly depended on the SZA and varied with altitude, with largest errors in the bottom part of the profile. Further identification of and correction for the errors observed and presented in this paper is currently under investigation and

beyond the scope of this paper. That study will also investigate how much the intercomparison results depend on the chosen retrieval algorithm, and hence compare the results of the different GOME retrieval schemes currently available (see section 1).

[57] The KNMI-GOME ozone profile also needs to be characterized by means of interpretation of the total data product, including averaging kernels and a priori data. We calculated the resolving length, which is one of several ways to estimate the resolution of the averaging kernels. This method is quite consistent with other definitions, but has the advantage that it gives sensible values over the whole altitude range. The average resolving length above 17-km altitude is about 11.3 ± 2.6 km. Below 17 km, the rapid increase of the resolving length indicates that the current GOME retrieval is not very sensitive to ozone values close to the reported altitude in this range.

[58] Investigation of the centroid of the averaging kernels supports the limitations of the GOME ozone profiles based on the resolving length. Below 20-km altitude, the centroids are shifted with respect to their nominal altitude. However, the centroids of 20 km and higher are well centered on their nominal altitude.

[59] Another aspect of the retrieval is the mixture of true and a priori information in the product. In the retrieved product below 20-km altitude very little new information has been added, and at these altitudes the a priori fraction forms on average more than two thirds of the product. Above 20-km altitude, the a priori fraction slowly decreases to about 50%, and at the highest layer it is only 10%.

[60] The above mentioned three interpretation parameters basically characterize the product. They indicate three features of the retrieval system, namely how well it is capable of resolving structures, how much information actually originates from the reported altitude, and how much measured information has actually been added. For a quick interpretation of a GOME ozone profile, we propose to report these three parameters for each altitude level. These tools can also be applied to other algorithms using the optimal estimation method (e.g., *Munro et al.* [1998], *Hoogen et al.* [1999], and *Connor et al.* [1991]), or for those algorithms only producing averaging kernels in their product (e.g., *Hasekamp and Landgraf* [2001]) the resolving lengths and the centroids of these kernels can be derived. Note that these tools are not necessarily restricted to only interpret GOME ozone profiles, and they can also be applied for the interpretation of, for example, microwave radiometer data.

[61] Applying these tools to the GOME data presented here, we conclude that the current retrieval scheme retrieves ozone values below 17-km altitude which should only be used with appropriate use of averaging kernels. This conclusion is based on a rapidly decreasing resolution, a shifting of the centroid away from its nominal altitude, and a substantial a priori fraction. Above 17 km up to 50 km the GOME spectra contain useful profile information, but the retrieved profiles have a moderate vertical resolution of about 11 km and contain a substantial fraction of a priori information of about 50%. This range interval, where we can expect the best results of the retrieval algorithm, almost completely overlaps with the altitude range of the lidar data,

demonstrating the appropriateness of using this data in GOME intercomparison and validation studies.

[62] **Acknowledgments.** We are grateful to R. D. Evans of NOAA for providing us the Dobson total ozone column density data, which were measured at NIWA Lauder, New Zealand within the NDSC. We also appreciated the availability of NCEP data from NOAA that were received from the NWS/Climate Prediction Center. This research was partly funded by a grant from the User Support Programme managed by the programme bureau external research of the Space Research Organization Netherlands (PB-SRON).

References

- Backus, G. E., and J. F. Gilbert, Uniqueness in the inversion of inaccurate gross Earth data, *Philos. Trans. R. Soc. London*, 266, 123–192, 1970.
- Bhartia, P. K., R. D. McPeters, C. L. Mateer, L. E. Flynn, and C. Wellemeyer, Algorithm for the estimation of vertical ozone profiles from the backscattered ultraviolet technique, *J. Geophys. Res.*, 101, 18,793–18,806, 1996.
- Boyd, I. S., G. E. Bodeker, B. J. Connor, D. P. J. Swart, and E. J. Brinksma, An assessment of ECC ozonesondes operated using 1% and 0.5% KI cathode solutions at Lauder, New Zealand, *Geophys. Res. Lett.*, 25, 2409–2412, 1998.
- Brinksma, E. J., et al., Analysis of record low ozone values during the 1997 winter over Lauder, New Zealand, *Geophys. Res. Lett.*, 25, 2785–2788, 1998.
- Brinksma, E. J., et al., Validation of 3 years of ozone measurements over Network for the Detection of Stratospheric Change station Lauder, New Zealand, *J. Geophys. Res.*, 105, 17,291–17,306, 2000.
- Brinksma, E. J., J. Ajtic, J. B. Bergwerff, G. E. Bodeker, I. S. Boyd, J. F. de Haan, W. Hogervorst, J. W. Hovenier, and D. P. J. Swart, Five years of observations of ozone profiles over Lauder, New Zealand, *J. Geophys. Res.*, 107(D14), 4216, doi:10.1029/2001JD000737, 2002.
- Burrows, J. P., et al., The Global Ozone Monitoring Experiment (GOME): Mission concept and first scientific results, *J. Atmos. Sci.*, 56, 151–175, 1999.
- Chance, K. V., J. P. Burrows, D. Perner, and W. Schneider, Satellite measurements of atmospheric ozone profiles, including tropospheric ozone, from ultraviolet/visible measurements in the nadir geometry: A potential method to retrieve tropospheric ozone, *J. Quant. Spectrosc. Radiat. Transfer*, 57, 467–476, 1997.
- Connor, B. J., A. Parrish, and J.-J. Tsou, Detection of stratospheric ozone trends by ground-based microwave observations, *Proc. SPIE Int. Soc. Opt. Eng.*, 1491, 218–230, 1991.
- Connor, B. J., G. E. Bodeker, R. L. McKenzie, and I. S. Boyd, The total ozone anomaly at Lauder, New Zealand, in 1997, *Geophys. Res. Lett.*, 26, 189–192, 1999.
- Fortuin, J. P. F., and H. Kelder, An ozone climatology based on ozonesonde and satellite measurements, *J. Geophys. Res.*, 103, 31,709–31,734, 1998.
- Hasekamp, O. P., and J. Landgraf, Ozone profile retrieval from backscattered ultraviolet radiances: The inverse problem solved by regularization, *J. Geophys. Res.*, 106, 8077–8088, 2001.
- Hasekamp, O. P., J. Landgraf, and R. van Oss, The need of polarization modeling for ozone profile retrieval from backscattered sunlight, *J. Geophys. Res.*, 107(D23), 4692, doi:10.1029/2002JD002387, 2002.
- Hoogen, R., V. V. Rozanov, and J. P. Burrows, Ozone profiles from GOME satellite data: Algorithm description and first validation, *J. Geophys. Res.*, 104, 8263–8280, 1999.
- McDermid, I. S., et al., OPAL: Network for detection of stratospheric change ozone profiler assessment at Lauder, New Zealand: 1. Blind intercomparison, *J. Geophys. Res.*, 103, 28,683–28,692, 1998a.
- McDermid, I. S., et al., OPAL: Network for detection of stratospheric change ozone profiler assessment at Lauder, New Zealand: 2. Intercomparison of revised results, *J. Geophys. Res.*, 103, 28,693–28,699, 1998b.
- Müller, M. D., A. K. Kaifel, M. Weber, S. Tellmann, J. P. Burrows, and D. Loyola, Ozone profile retrieval from Global Ozone Monitoring Experiment (GOME) data using a neural network approach (Neural Network Ozone Retrieval System (NNORSY)), *J. Geophys. Res.*, 108(D16), 4497, doi:10.1029/2002JD002784, 2003.
- Munro, R., R. Siddans, W. J. Reburn, and B. J. Kerridge, Direct measurements of tropospheric ozone distributions from space, *Nature*, 392, 168–171, 1998.
- Rodgers, C. D., Characterization and error analysis of profiles retrieved from remote sounding measurements, *J. Geophys. Res.*, 95, 5587–5595, 1990.
- Rodgers, C. D., *Inverse Methods For Atmospheric Sounding, Theory and Practice*, vol. 2, *Atmos. Oceanic Planet. Phys. Ser.*, World Sci. Publ., Singapore, 2000.
- Spurr, R. J. D., Linearized radiative transfer theory: A general discrete ordinate approach to the calculation of radiances and analytic weighting functions, with application to atmospheric remote sensing, Ph.D. thesis, Tech. Univ. Eindhoven, Netherlands, 2001.
- Stratospheric Processes and Their Role in Climate (SPARC), Assessment of trends in the vertical distribution of ozone, in *SPARC Rep. 1*, edited by N. Harris, R. Hudson, and C. Phillips, World Meteorol. Organ., Geneva, Switzerland, 1998.
- van der A, R. J., R. F. van Oss, and H. M. Kelder, Ozone profile retrieval from GOME data, in *Satellite Remote Sensing of Clouds and the Atmosphere III*, edited by J. E. Russell, *Proc. SPIE Int. Soc. Opt. Eng.*, 3495, 221–229, 1998.
- van der A, R. J., R. F. van Oss, A. J. M. Piters, J. P. F. Fortuin, Y. J. Meijer, and H. M. Kelder, Ozone profile retrieval from recalibrated Global Ozone Monitoring Experiment data, *J. Geophys. Res.*, 107(D15), 4239, doi:10.1029/2001JD000696, 2002.

P. V. Johnston, National Institute of Water and Atmospheric Research, PB 50061, Omakau 9182, Central Otago, New Zealand. (p.johnston@niwa.co.nz)

H. M. Kelder, R. J. van der A, and R. F. van Oss, Section Atmospheric Composition, Department of Climate Research and Seismology, Royal Netherlands Meteorological Institute, P.O. Box 201, 3730 AE De Bilt, Netherlands. (kelder@knmi.nl; avander@knmi.nl; ossvanr@knmi.nl)

Y. J. Meijer and D. P. J. Swart, Laboratory for Environmental Measurements, Environmental Risks and Safety Division, National Institute of Public Health and the Environment, P.O. Box 1, A. van Leeuwenhoeklaan 9, Bilthoven, Utrecht 3720 BA, Netherlands. (yasjka.meijer@rivm.nl; daan.swart@rivm.nl)